ORGANIC LETTERS

2008
Vol. 10, No. 24
5561−5564

3,3′- and 4,4′-Biphenylene-Bridged Subporphyrin Dimers

Yasuhide Inokuma and Atsuhiro Osuka*

Department of Chemistry, Graduate School of Science, Kyoto University Sakyo-ku, Kyoto 606-8502, Japan

osuka@kuchem.kyoto-u.ac.jp

Received October 16, 2008

ABSTRACT

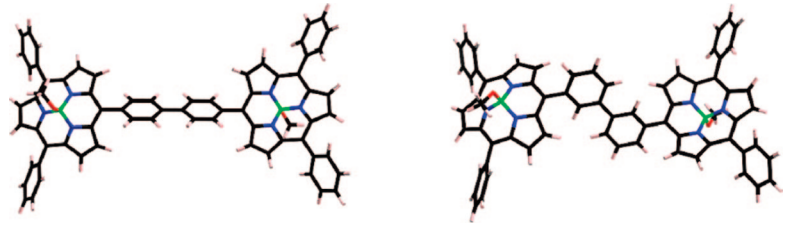

3,3′- and 4,4′-biphenylene-bridged subporphyrin dimers were synthesized by means of a Ni-catalyzed homocoupling reaction. Distinctly red-shifted absorption bands and enhanced fluorescence were observed only for the latter, indicating effective through-bond interactions through a 4,4′-biphenylene bridge, which is not possible for porphyrins.

Subporphyrin is a genuine contracted porphyrin that possesses a curved 14π-aromatic circuit along a bowl-shaped structure. The chemistry of subporphyrin was triggered by our first synthesis of tribenzosubporphine in 2006.[1] Since then, a variety of periphery-substituted[2] and core-modified[3] analogues have been explored which display fascinating properties such as intense green fluorescence and large *meso*-aryl-substituent effects on the electrochemical and optical properties. A promising next step will be to explore covalently linked subporphyrin oligomers, but only two examples have been reported so far, which are both constructed by axial coordination at the boron atom.[2b,4] This present situation of subporphyrins is clearly different from that of subphthalocyanines[5] in that various covalently linked subphthalocyanine dimers and trimers have been synthesized and shown to exhibit interesting electronic properties.[6] In this context, the interchromophore interactions in covalently linked subporphyrin oligomers still remain virtually unexplored. Herein, we wish to report the synthesis of 3,3′- and 4,4′-biphenylene-bridged subporphyrin dimers as the first examples of aromatic-bridged subporphyrin oligomers.

Scheme 1 outlines the synthetic route of biphenylene dimers **1** and **2**. Pyridine−tri-*N*-pyrrolylborane, benzaldehyde, and 4-bromobenzaldehyde were condensed in the presence of trifluoroacetic acid followed by aerobic refluxing in 1,2-dichlorobenzene to give a mixture of four possible subporphyrins. This mixture was dissolved in DMF and heated to 80 °C in the presence of $NiCl_2$(dppp), Zn powder, and KI to afford 4,4′-biphenylene-linked dimer **1** in 1.3%

(1) Inokuma, Y.; Kwon, J. H.; Ahn, T. K.; Yoon, M.-C.; Kim, D.; Osuka, A. *Angew. Chem., Int. Ed.* **2006**, *45*, 961–964.

(2) (a) Kobayashi, N.; Takeuchi, Y.; Matsuda, A. *Angew. Chem., Int. Ed.* **2007**, *46*, 758–760. (b) Takeuchi, Y.; Matsuda, A.; Kobayashi, N. *J. Am. Chem. Soc.* **2007**, *129*, 8271–8281. (c) Inokuma, Y.; Yoon, Z. S.; Kim, D.; Osuka, A. *J. Am. Chem. Soc.* **2007**, *129*, 4747–4761. (c) Makarova, E. A.; Shimizu, S.; Matsuda, A.; Luk'yanets, E. A.; Kobayashi, N. *Chem. Commun.* **2008**, 2109–2111. (d) Tsurumaki, E.; Inokuma, Y.; Easwaramoorthi, S.; Lim, J. M.; Kim, D.; Osuka, A. *Chem.—Eur. J.*, in press (DOI: 10.1002/chem.200801802).

(3) Myśliborski, R.; Latos-Grażyński, L.; Szterenberg, L.; Lis, T. *Angew. Chem., Int. Ed.* **2006**, *45*, 3670–3674.

(4) Inokuma, Y.; Osuka, A. *Chem. Commun.* **2007**, 2930–2940.

(5) (a) Meller, A.; Ossko, A. *Monatsh. Chem.* **1972**, *103*, 150–155. (b) Claessens, C. G.; Gonzalez-Rodriguez, D.; Torres, T. *Chem. Rev.* **2002**, *102*, 835–853. (c) Torres, T. *Angew. Chem., Int. Ed.* **2006**, *45*, 2834–2837.

(6) (a) Claessens, C. G.; Torres, T. *Angew. Chem., Int. Ed.* **2002**, *41*, 2561–2565. (b) Fukuda, T.; Stork, J. R.; Potucek, R. J.; Olmstead, M. M.; Noll, B. C.; Kobayashi, N.; Durfee, W. S. *Angew. Chem., Int. Ed.* **2002**, *41*, 2565–2568. (c) Iglesias, R. S.; Claessens, C. G.; Torres, T.; Herranz, M. A.; Ferro, V. R.; Garcı´a de la Vega, J. M. *J. Org. Chem.* **2007**, *72*, 2967–2977. (d) Igleslas, R. S.; Claessens, C. G.; Herranz, M. A.; Torres, T. *Org. Lett.* **2007**, *9*, 5381–5384.

10.1021/ol8023924 CCC: $40.75
Published on Web 11/19/2008

yield for two steps along with triphenylsubporphyrin **3** (2.4%). 3,3′-Biphenylene-bridged subporphyrin dimer **2** was also prepared by the same procedure from 3-bromobenzaldehyde in 1.0% yield. The parent ion peak was observed at $m/z = 969.3696$ for **1** (calcd for $C_{67}H_{43}N_6B_2O_1 = 969.3699$ $[M - OMe]^+$), while two peaks were detected for **2** at $m/z = 969.3694$ and 1023.3789 (calcd for $C_{68}H_{46}N_6B_2O_2Na = 1023.3781$ $[M + Na]^+$) by ESI-TOF mass analysis. The ^1H NMR spectrum of **1** exhibits a single set of subporphyrin signals featuring a singlet at 8.15 ppm and a couple of doublets at 8.26, 8.18 ppm due to β-protons and a singlet at 0.89 ppm due to the axial methoxyl protons. Observation of the protons in the 4,4′-biphenylene bridge as a pair of doublets at 8.27 and 8.14 ppm indicates its free rotation at room temperature. A similar ^1H NMR spectral pattern was recorded for 3,3′-linked dimer **2**, thus suggesting that two subporphyrin subunits are equivalent in both **1** and **2**.

Scheme 1. Synthesis of Biphenylene-Linked Dimers **1** and **2**

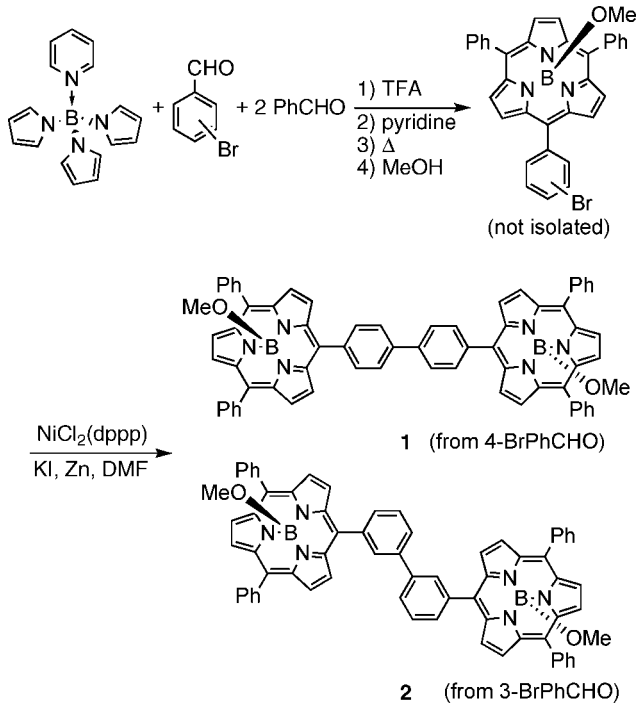

Single-crystal X-ray diffraction analysis revealed the solid-state structure of **1** (Figure 1)[7] in which the two axial methoxy groups are pointed at the opposite direction, as can be seen in the side view, and hence takes C_i molecular symmetry. The B−B′ distance is 15.9 Å, and the C5−C5′ (two *meso*-carbons at the linkage) distance is 10.1 Å. The two bowl-shaped cores are arranged in a wavelike form. Interestingly, the 4,4′-biphenylene subunit displays a rather coplanar conformation with a dihedral angle of 50.9° toward the subporphyrin mean plane. These structural features are favorable for the effective through-bond interaction of two subporphyrin chromophores.

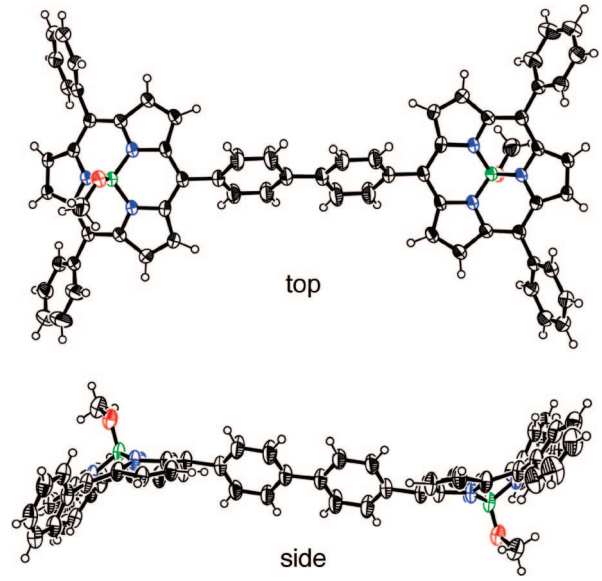

Figure 1. ORTEP representations of the crystal structure of **1** drawn at the 50% probability level (black, carbon; red, oxygen; blue, nitrogen; green, boron).

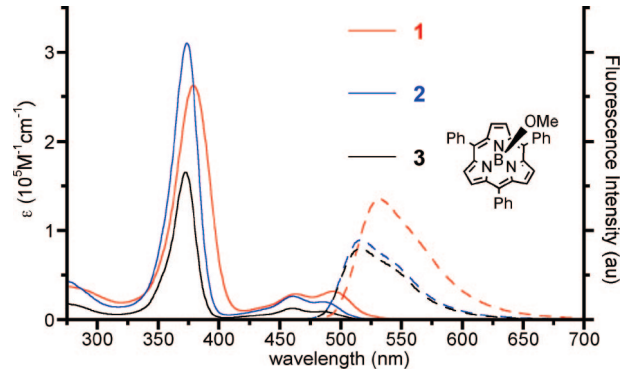

Figure 2. UV−vis absorption (solid line) and fluorescence (dashed line) spectra of subporphyrins in CH_2Cl_2.

Figure 2 shows UV−vis absorption and fluorescence spectra of **1**−**3** in CH_2Cl_2. The absorption spectrum of **1** differs substantially from those of **2** and **3**. The dimer **2** shows a Soret-like band at 374 nm and Q-like bands at 461 and 486 nm, which is similar to that of the parent *meso*-triphenyl-substituted subporphyrin **3**. Thus, the absorption spectrum of **2** can be roughly reproduced by the summation of that of **3**, which indicates merely weak electronic interaction between the two subporphyrin units in the ground state. In contrast, the dimer **1** shows a definitely red-shifted Soret-like band at 379 nm and Q-like bands at 463 and 494 nm along with slight but distinct broadening. In addition, the Q(0,0) band of **1** is enhanced compared to Q(1,0)

(7) Crystall data for **1**: $C_{68}H_{48}B_2N_6O_2{\cdot}CH_2Cl_2$, $M = 1085.65$, monoclinic, space group $P2_1/c$ (no. 14), $a = 11.866(4)$ Å, $b = 19.05(7)$ Å, $c = 12.211(5)$ Å, $\beta = 103.446(15)°$, $V = 2748.9(17)$ Å^3, $Z = 2$, $D_{calc} = 1.312$ g cm^{-3}, $R_1 = 0.0822$ for $I > 2\sigma(I)$, $wR = 0.2784$ for all data, CCDC 705219.

transition, which also contrasts to the usual spectral feature of *meso*-aryl substituted subporphyrins as seen in **2** and **3**.

The enhanced electronic interactions of **1** can be seen also in the fluorescence. The dimer **2** emits green fluorescence at 516 nm with its quantum yield (Φ_F) of 0.15, which is comparable to that of **3** ($\Phi_F = 0.13$). On the other hand, the dimer **1** exhibits yellowish-green fluorescence at 531 nm tailing over 650 nm as a good mirror image of Q(0,0) band. Interestingly, the fluorescence quantum yield of **1** ($\Phi_F = 0.28$) is ca. 2-fold of **3**.

To confirm the enhanced electronic interactions in **1**, the electrochemical properties of **1**−**3** were examined by cyclic voltammetry, which also revealed a distinctly different property of **1** from those of **2** and **3** (Table 1 and Supporting Information). The first oxidation and reduction waves of **2** were observed at 0.81 and −1.91 V (vs ferrocene/ferrocenium ion couple) both as reversible processes. On the basis of these results, the electrochemical HOMO−LUMO gap of **2** has been estimated to be 2.72 eV, which is similar to that of monomer **3** (2.68 eV). On the other hand, the dimer **1** shows two reversible oxidation waves at 0.61 and 0.75 V. The first oxidation potential of **1** is remarkably lower than those of **2** and **3**, although the reduction potential of **1** is similar to **2** and **3**. As a consequence, the HOMO−LUMO gap of **1** is ca. 0.15 V smaller than **2** and **3**, which is in good agreement with optical HOMO−LUMO gaps (2.51, 2.55, and 2.56 eV for **1**, **2**, and **3**, respectively).

Table 1. Redox Potentials[a] and Electrochemical HOMO−LUMO Gaps of **1**−**3**

	$E^2_{ox,1/2}$	$E^1_{ox,1/2}$	$E^1_{red,1/2}$	HOMO−LUMO gap
1	0.75	0.61	−1.93	2.54
2		0.81	−1.91	2.72
3		0.71	−1.97	2.68

[a] Values are reported in V vs ferrocene/ferrocenium ion couple. Measurement conditions: solvent, CH_2Cl_2 with 0.10 M Bu_4NPF_6 as a supporting electrolyte; working electrode, glassy carbon; counter electrode, platinum; reference electrode, $Ag/AgClO_4$.

Molecular orbital calculations of **1** and **2** were performed with the Gaussian 03 package[8] at the B3LYP/6-31G* level on the basis of the crystal structure and the optimized structure, respectively. In the optimized structure, the dimer **2** takes a relatively planar conformation with a B−B′ distance of 14.5 Å. Interestingly, HOMO and LUMO of **1** show large orbital coefficients on the biphenylene bridge, whereas those of **2** are vanishingly small at the bridge, suggesting efficient and inefficient elongation of π-conjugation for 4,4′- and 3,3′-biphenylene linkages, respectively. The HOMO−LUMO gaps of **1**, **2**, and **3** were calculated to be 2.94, 3.17, and 3.18 eV, respectively, showing a certain decrease for **1** in accord with the experimental results. In the case of biphenylene-bridged porphyrin dimers,[9] the dihedral angle between the biphenylene linker and porphyrin mean plane is roughly perpendicular. This leads to small through-bond interactions between two porphyrins in the ground state. On the other hand, 4,4′-biphenylene bridge in **1** can serve as a conjugated linker which enables strong orbital interactions between two subporphyrins. Consequently, a 4,4′-biphenylene subunit can provide remarkable through-bond interaction for the subporphyrin case.

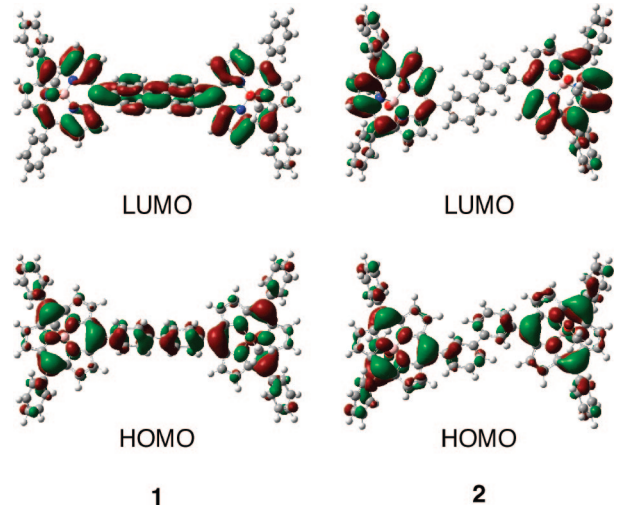

Figure 3. Frontier molecular orbitals of **1** and **2** calculated at the B3LYP/6-31* level.

While the B−B′ distance in **1** is fixed, that of **2** can change upon bond rotation. Since axially coordinated boron ligand can be changed reversibly by carboxyl groups,[2,4] we examined axial ligand exchange reaction with biphenyl-3,3′-dicarboxylic acid (**4**) to form a 1:1 cyclic complex, **5**, in which the distance and arrangement of two subporphyrins are fixed. A 1:1 mixture of **2** and **4** was refluxed in toluene under diluted conditions (~125 μM). After removal of the solvent, complex **5** was obtained quantitatively. The ESI-TOF mass spectrum of **5** exhibits its parent cation peak at $m/z = 1179.4028$, which is calculated for $C_{80}H_{49}N_6B_2O_4 = 1179.4019$ [**2** − 2 × MeOH + **4**]$^+$. The ^{1}H NMR spectrum also supports the cyclic structure of **5**, featuring C_2 symmetric signal pattern and shielded signals at 6.7−7.0 ppm due to axial ligand. The highly deshielded singlet at 9.28 ppm is assigned to the biphenylene bridge proton (H^a in Scheme 2), and this characteristic shift is attributed to the diatropic ring current of the two subporphyrins forced in a face-to-face conformation.

The dihedral angle of two subporphyrins' mean plane is 88° for **5**, and the boron−boron distance is kept distinctly short (10.3 Å) (Supporting Information). UV−vis absorption spectrum of **5** recorded in CH_2Cl_2 was, however, almost identical to that of **2**, exhibiting absorption maxima at 371, 458, and 481 nm. Although the center-to-center interchromophore distances of **2** and **5** are considerably shorter than **1**, perturbations observed in their UV−vis absorption spectra

(8) For the full citation, see the Supporting Information.

(9) Cho, S.; Yoon, M.-C.; Kim, C. H.; Aratani, N.; Mori, G.; Joo, T.; Osuka, A.; Kim, D. *J. Phys. Chem. C* **2007**, *111*, 14881–14888.

are negligible. These facts indicate the importance of the through-bond interaction in **1**.

Scheme 2. Axial Ligand Exchange Reaction of **2** and ^{1}H NMR Spectra of **2** and **5** in $CDCl_3$ (*: Solvent Peak)

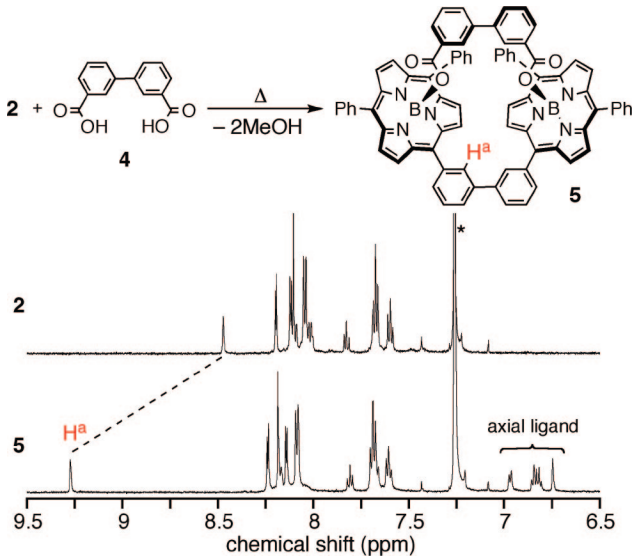

In summary, we have prepared biphenylene-bridged subporphyrin dimers **1** and **2** by a Ni-catalyzed homocoupling reaction as the first example of an aromatic-bridged subporphyrin dimer. Cyclic dimer **5** was also synthesized from **2** and dicarboxylic acid **4** as a distance- and orientation-fixed model. 4,4′-Biphenylene-bridged dimer **1** exhibited a bathochromically shifted absorption spectrum, intensified fluorescence emission, and a distinctly reduced HOMO−LUMO gap as revealed by the electrochemical and computational studies, whereas such perturbations were only marginal for **2** and **5** in spite of their shorter interchromophore distances compared to **1**. Therefore, the distinctly perturbed characteristics of **1** can be ascribed to the effective π-conjugation through a 4,4′-biphenylene unit which is difficult for porphyrins. It can be concluded that through-bond interaction assisted by the conjugation bridge is particularly important for interchromophore communication between two subporphyrins.

Acknowledgment. This work was supported by a Grant-in-Aid (A) (No. 19205006) for Scientific Research from MEXT. Y.I. thanks the JSPS Research Fellowship for Young Scientists.

Supporting Information Available: Experimental procedures and spectroscopic data for new compounds and crystal data of **1** (CIF). This material is available free of charge via the Internet at http://pubs.acs.org.

OL8023924